

# Joint Two-Dimensional Observations of Ground Magnetic and Ionospheric Electric Fields Associated with Auroral Zone Currents

## 3. Auroral Zone Currents During the Passage of a Westward Travelling Surge

B. Inhester<sup>1\*</sup>, W. Baumjohann<sup>1</sup>, R.A. Greenwald<sup>2\*\*</sup>, and E. Nielsen<sup>2</sup>

<sup>1</sup> Institut für Geophysik der Universität Münster, D-4400 Münster, Federal Republic of Germany

<sup>2</sup> Max-Planck-Institut für Aeronomie, D-3411 Katlenburg-Lindau 3, Federal Republic of Germany

**Abstract.** Ground magnetic perturbations and ionospheric electric fields have been observed by the Scandinavian Magnetometer Array and the STARE radars, respectively, during the passage of a westward travelling surge in the late evening sector. On the basis of these measurements, the three-dimensional current system in the vicinity of the westward travelling surge is modelled. The results support a current model recently proposed by Rostoker and co-workers on the basis of purely magnetic ground-based measurements. In particular, we can identify an upward field-aligned current of about  $5 \times 10^4$  A in the head of the surge. Ahead of the surge, we find a south-eastward directed electric field. Additionally, we have some evidence for the existence of a south-westward directed electric field east of the surge. The latter may be explained by the generation of polarisation charges at the northern and southern boundaries of the higher conducting region east of the surge's head.

**Key words:** Scandinavian Magnetometer Array – STARE radars – Westward travelling surge – Current system modelling

### Introduction

In today's understanding of polar ionospheric physics, the *westward travelling surge* (WTS) is regarded as the optical signature of the expansion of magnetospheric substorm energy from the midnight into the evening sector. During the expansive phase of a substorm (Akasofu 1964), energy is released in the form of intensification of auroral arcs and ionospheric electrical currents in the midnight sector. From here, the zone of intensified westward currents spreads into the evening sector along the auroral zone. The propagating head of the enhanced westward electrojet is thought to coincide spatially with the fold of the WTS (Akasofu et al. 1966, 1969).

Kisabeth and Rostoker (1973), Rostoker and Hughes (1979), and Tighe and Rostoker (in press 1981) have studied models for the ionospheric current flow associated with a surge and compared

them with ground magnetic perturbations, measured along a chain of magnetometers. They found a localised, positive *D* deflection in the magnetic variations to be characteristic of the passage of westward travelling surges and explained it by an area of southward ionospheric current travelling together with the auroral form. As a consequence of their model current system, Rostoker and Hughes (1979) predicted an eastward component of the ionospheric electric field at the head of the surge. They assumed a westward electric field behind the surge in agreement with electric field measurements carried out with the Chatanika incoherent scatter radar (Banks et al. 1973; Horwitz et al. 1978).

In the present paper we present data of ground magnetic perturbations and ionospheric electric fields, measured simultaneously in the vicinity of a WTS that crossed northern Scandinavia on 27 March 1977 at approximately 19:00 UT (about 21 MLT). Both magnetic perturbations and electric fields have been measured in a two-dimensional, horizontal plane. In earlier studies of this series (Baumjohann et al. 1980, in press 1981; Baumjohann and Kamide in press 1981) it has already been shown that the simultaneous two-dimensional observations of ground magnetic and ionospheric electric fields have basic advantages over previous observations when studying the three-dimensional current flow associated with auroral electrojets. In this paper we will see that simultaneous two-dimensional measurements help even more when one attempts to understand the highly inhomogeneous and localised current system associated with a westward travelling surge.

In the following we describe the temporal and spatial variations of magnetic and electric fields during the passage of the WTS and, on the basis of those measurements, we model ionospheric and field-aligned currents and height-integrated ionospheric conductivities and discuss the model in the context of previously proposed models.

### Instrumentation

The ground magnetic disturbance and ionospheric electric fields have been observed by the two-dimensional *Scandinavian Magnetometer Array* (SMA) and the *Scandinavian Twin Auroral Radar Experiment* (STARE), respectively. In addition, magnetograms from observatories at Ny Ålesund and Bjørnøya were included in this study. Optical recordings of the WTS have been performed by all-sky cameras at Ivalo and in Abisko. A detailed description of the SMA is given by Maurer and Theile (1978) and Küppers

### Present addresses:

\* Max-Planck-Institut für Aeronomie, D-3411 Katlenburg-Lindau 3, Federal Republic of Germany

\*\* Applied Physics Laboratory, Johns Hopkins University, Laurel, MD 20810, USA

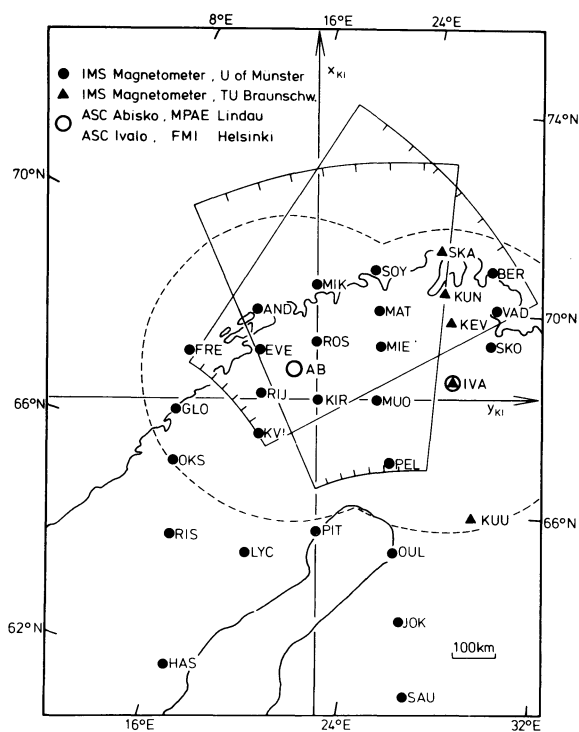


Fig. 1. Locations of the magnetic stations used in this study. The trapezoids define the observation areas of the two STARE radars. The observational coverage of the two all-sky cameras used in this study is indicated by the broken circles (as defined by  $70^\circ$  zenith angle at 110 km height). The axes define the Kiruna system (see text)

et al. (1979). For the STARE-radars, we refer to Greenwald et al. (1978).

The locations of the magnetometers and all-sky cameras, together with the approximate observation area of the latter at 110 km altitude (for a maximum zenith angle of  $70^\circ$ ) are shown in Fig. 1. The figure also illustrates the observation area of the two STARE radar antennas, situated at Malvik, near Trondheim, Norway and Hankasalmi, Finland, near the magnetometer station SAU.

The STARE radars measure the Doppler shift of radar signals scattered by plasma waves in the auroral  $E$  region (Farley 1963; Rogister and D'Angelo 1970). The combination of the Doppler shifts from both STARE radars give the plasma wave phase velocity perpendicular to the earth's magnetic field with a spatial resolution of roughly  $20 \times 40 \text{ km}^2$ . There is strong experimental and theoretical evidence that the phase velocity measured coincides with the  $\mathbf{E} \times \mathbf{B}$  - drift of  $E$  region electrons (Farley 1963; Rogister and D'Angelo 1970; Ecklund et al. 1977; Cahill et al. 1978). Hence the ionospheric electric field perpendicular to the earth's magnetic field can be derived. In order to observe auroral zone electric fields with this type of radar the electric field must exceed a threshold value in order to excite the plasma irregularities. Cahill et al. (1978) found threshold values of 15–20 mV/m for the STARE radars. In regions where appreciable ionospheric currents are due primarily to high conductivities rather than high electric fields, as for example in auroral arcs (Evans et al. 1977), one will not observe radar auroral backscatter if the electric fields are below the threshold.

The coordinate system in Fig. 1 and in all the other maps in this paper is the Kiruna system of Küppers et al. (1979). The

$x_{KI}$  axis of this system is chosen perpendicular to the revised corrected geomagnetic latitude circle (Gustafsson 1970) through Kiruna, Sweden, and points approximately  $12^\circ$  west of geographic north. The magnetic disturbance and the irregularity drift vectors have been transformed into the Kiruna system as described by Küppers et al. (1979). The horizontal components of the magnetic disturbance in this system are denoted by  $A$  (along  $x_{KI}$ , approximately north) and  $B$  (along  $y_{KI}$ , approximately east). The auroral structures in the all-sky camera pictures have also been mapped into the Kiruna system under the assumption that their lower border is at a mean altitude of 110 km (Boyd et al. 1971).

## Observations

On 27 March 1977 a weak substorm commenced in the midnight sector at 19:00 UT. The magnetometer stations at Kharasavey and Tambey on  $145^\circ$  geomagnetic longitude recorded a sharp 100 nT decrease in the  $H$  component at that time (A.N. Zaitsev, private communication). About 15 min later, a WTS passed over northern Scandinavia, its head travelling with a speed of roughly  $800 \text{ ms}^{-1}$ .

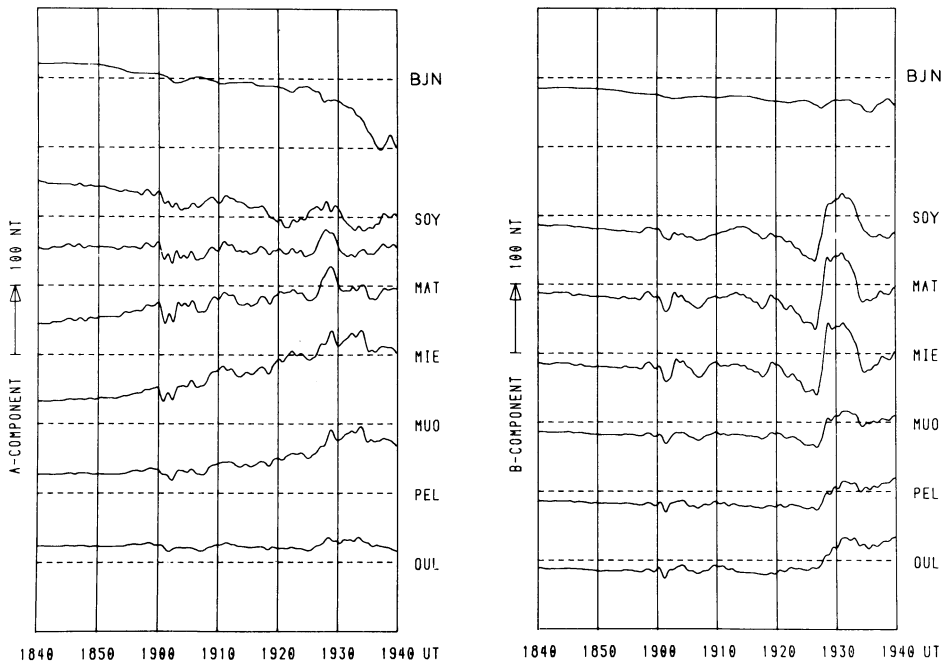
Magnetograms from the latitudinal line of magnetometers ranging from station OUL to SOY (see Fig. 1) and BJN (about 500 km north of SOY), are shown in Fig. 2. They are governed by a southward moving eastward electrojet before the onset at 19:00 UT. Afterwards, the eastward electrojet intensifies but the influence of the simultaneously growing westward electrojet keeps the  $A$  component of the northernmost stations SOY and MAT from exhibiting large deflections. The passage of the WTS is indicated in the  $B$  component by a small peak of 15 nT, embedded in the general substorm variation.

Figure 3 shows the irregularity drift pattern and the ground equivalent current vectors observed during the passage of the WTS for three successive instances of time. A remarkable similarity between the irregularity flow direction and the auroral structures can be seen as soon as the WTS enters the field of view of the STARE antennas. In the immediate vicinity of the auroral luminosity an irregularity drift that is more or less parallel to the auroral form can be found. Hence, the electric field is perpendicular to the auroral structures, as is expected if electrons precipitate strongly into the auroral form. No irregularity drift could be measured in the region east of the surge's fold due, probably, to a sub-threshold electric field in this region. As mentioned above, the irregularity drift vectors can be identified with the  $\mathbf{E} \times \mathbf{B}$  - drift of ionospheric electrons. Hence, lines of constant electric potential in the plane of the ionosphere coincide with the flow lines of the irregularity drift vector field. Apparently, the auroral form coincides approximately with one of those equipotential lines. If this potential contour were to be extrapolated into the region east of the WTS, where no irregularity drift is detected, a weak southward and westward irregularity flow could be assumed in this region. This assumption is supported by the observation of westward electric fields, or southward electron drifts after the passage of a WTS using the incoherent scatter technique (Horwitz et al. 1978).

The ground equivalent current pattern in the lower part of Fig. 3 is more difficult to relate to the auroral structure, as it is governed by the eastward electrojet flowing south of the surge. Unfortunately, the surge passes along the Scandinavian coastline and the magnetic measurements do not cover the area north of the WTS. Still, an enhancement of the westward component of the equivalent current near the northernmost stations is observable, after the head of the surge has passed, indicating the intrusion

77-03-27

77-03-27



**Fig. 2.** Magnetograms of  $A$  and  $B$  components on a latitudinal profile ranging from BJN (Bear Island) to OUL, on 3 March 1977.  $A$  and  $B$  are horizontal magnetic disturbance components along the  $x_{KI}$  and  $y_{KI}$  axes, respectively (see Fig. 1)

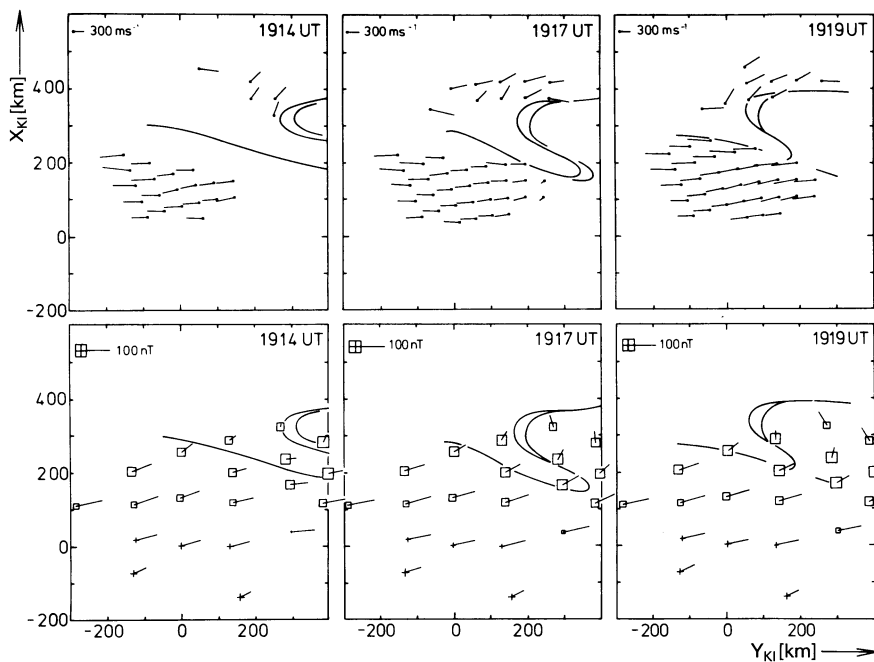


**Fig. 3.** Spatial distribution of irregularity drift vectors (*upper row*) and equivalent current vectors on the ground (*lower row*; squares and crosses denote negative and positive  $Z$  components, respectively) for three instances of time. Also shown are the digitised lower borders of the surge structure

of the westward electrojet. The pronounced positive  $D$  disturbance or southward equivalent current component immediately ahead of a WTS as found by Kisabeth and Rostoker (1973) is not seen in Fig. 3. Instead, there is an overall negative  $D$  or northward equivalent current component, that stays stable during the passage of the surge and is probably not related to the WTS.

After 19:20 UT, the auroral structures became barely detectable against the sunlit western horizon. However, as long as the surge can be traced on the all-sky camera pictures, it seems to maintain its shape, except for a slight de-folding, as can be seen in Fig. 3. In addition, the irregularity drift and equivalent current

vector fields obviously remain constant relative to the location of the surge. This suggests a stationary pattern for the WTS and the electric and magnetic perturbations related to it which drifts with the WTS. In order to display this behaviour clearly, the auroral luminosity structures and vector fields for the times of Fig. 3, including 19:11 UT, were superimposed on each other in the moving frame of the WTS. The result is shown in Fig. 4, where we have plotted electric fields instead of irregularity drifts and have removed the above mentioned stationary and homogeneous bias of  $-20$  nT in the  $B$  components. We did not include in the electric field the Lorentz-force due to the motion of our

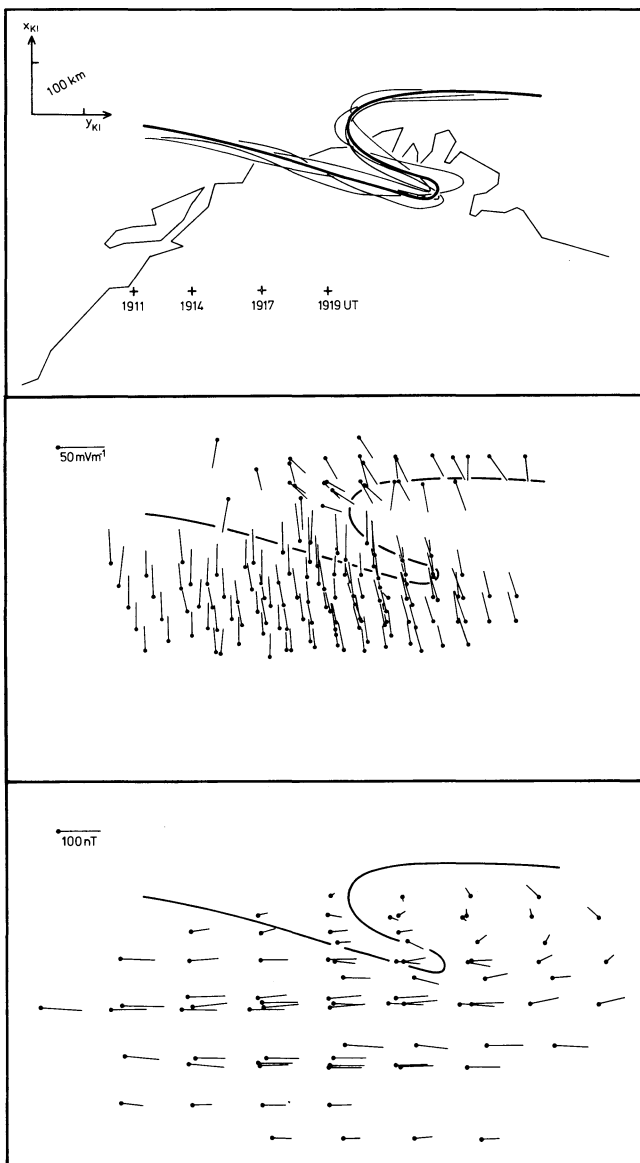


**Fig. 4.** Spatial distribution of electric field vectors (*middle panel*), equivalent current vectors on the ground (*lower panel*) and auroral luminosity structures (*upper panel*) for the times of Fig. 3 and 19:11 UT plotted one above the other under the assumption of a stationary pattern, drifting with the WTS (relative locations at different times are given by the + signs in the upper panel)

reference frame relative to the earth's magnetic field, because it is not the ionospheric plasma that moves with the surge, but rather the source of its luminosity.

Figure 4 demonstrates the basic results of our observations. The surge basically maintains its shape during the 8 min of its observation. In its vicinity, the electric field is modified to be normal to the auroral structure. The area around the WTS can be divided into three regions: northward directed electric fields south of the WTS, southward directed fields in the north and the west, with an increasing eastward component near the head of the surge. Presumably, a sub-threshold westward directed electric field is located in the fold east of the surge. The observed electric fields are in accord with incoherent scatter measurements (Banks et al. 1973; Horwitz et al. 1978), except that we see an

unusually large eastward electric field ahead of the surge as compared to the sub-threshold field behind it. In contrast, Banks et al. (1973) reported westward electric fields of  $15 \text{ mV m}^{-1}$  after the passage of a surge, while there was no enhancement of the eastward component ahead of the surge. From Fig. 4 it is seen that the area of eastward electric fields ahead of the surge has a longitudinal extent of only 100–200 km. Since the surge propagates with a typical speed of  $50 \text{ km min}^{-1}$ , a time resolution of better than 3 min would be needed for a radar to detect the eastward field region. Moreover, the radar-beam must be directed into the correct spatial region relative to the shape of the WTS. In the operating mode used by Banks et al. (1973) and Horwitz et al. (1978) the Chatanika incoherent scatter radar required more than 2 min integration time in order to give a reliable electric field value at one point. Thus it is quite probable that they were simply not looking in the right place at the right time in order to observe the eastward electric field ahead of the surge. On the other hand, incoherent scatter radars are not limited to observing electric fields above some threshold value, such as STARE is. So Banks et al. (1973) and Horwitz et al. (1978) were able to observe the region of weaker westward directed electric field behind the surge, which obviously must have had a greater longitudinal extent than the region of the eastward electric field.

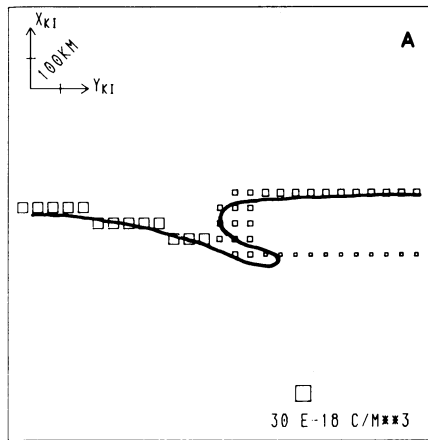
The equivalent current in our observations is dominated by the eastward electrojet flowing in the region of northward directed electric field south of the WTS. The influence of the advancing westward electrojet can be seen in the northeast. In the transition region, we find a slight southward current component immediately ahead of the surge, and an increasingly northward component of the ground equivalent current behind it. This behaviour in the north-south current flow is consistent with the observed peak in the  $B$  component that is seen in the magnetograms in Fig. 2 at that time, when the surge passes over the magnetometer profile. Kisabeth and Rostoker (1973) found this variation to be typical of a WTS passage, although the magnitude of the peak that we observed is small compared with their observations. On the other hand, above the region of positive  $B$  ground magnetic variation, there obviously exists an eastward electric field. This field may drive a southward Hall current giving rise to a strong positive  $B$  deflection, according to the model proposed by Rostoker and Hughes (1979). In order to resolve the effects quantitatively, estimates of the distribution of ionospheric conductivities relative to the surge must be included.

### Numerical Models

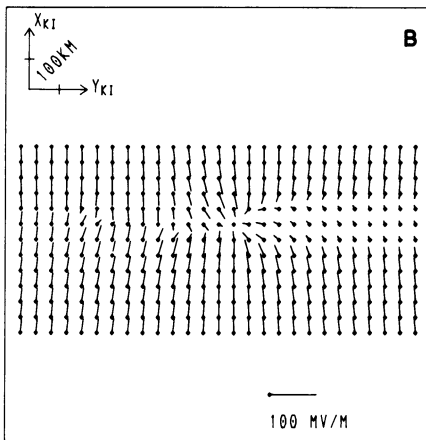
As has already been extensively discussed in the early papers of this series (Baumjohann et al. 1980 in press 1981; Baumjohann and Kamide in press 1981) it is possible to significantly restrict the large number of equivalent current systems that may fit ground magnetic disturbances. This is accomplished by combining two-dimensional measurements of the magnetic variations made by the SMA and ionospheric electric fields observed with STARE. In order to find a probable three-dimensional current system that is consistent with the ground magnetic variation and the ionospheric electric field measurements, we modelled the ionospheric current system numerically.

For the calculations, the ionospheric plane at 110 km height (Kamide and Brekke 1977) was divided into cells of  $50 \times 50 \text{ km}^2$  with a constant height-integrated conductivity, electric field and current density. The divergence of the horizontal currents between different cells gives the field-aligned current flow. The ground

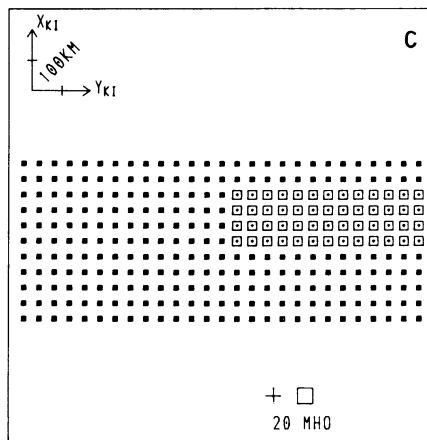
COLUMN CHARGES



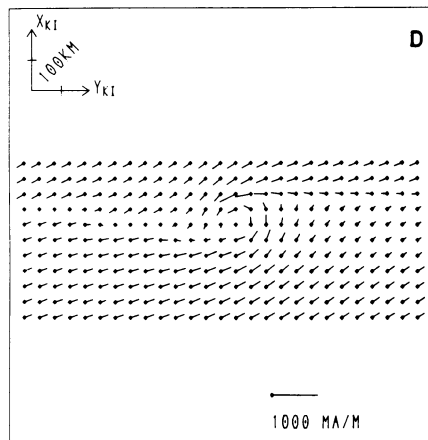
IONOSPHERIC ELECTRIC FIELD



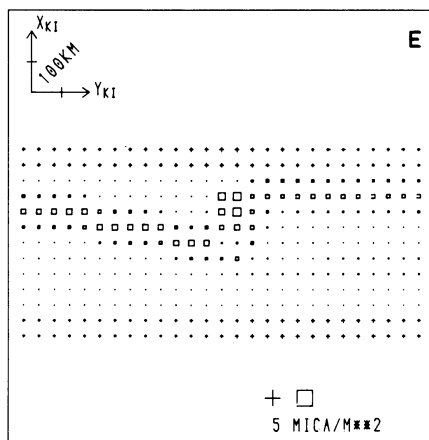
IONOSPHERIC CONDUCTIVITY



IONOSPHERIC CURRENTS



FIELD-ALIGN CURRENTS



EQ CURR GROUND

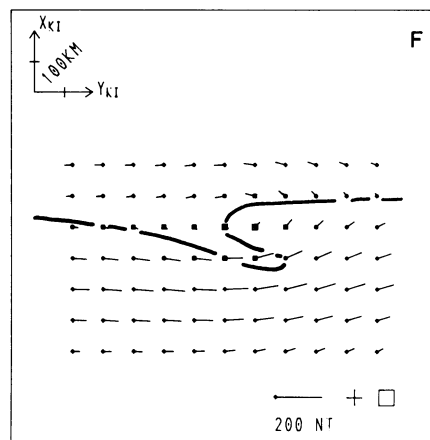


**Fig. 5a-f.** Parameters of the model current system A and resultant equivalent current vectors on the ground. **a** Distribution of field-aligned columns of negative electrical charges. **b** Ionospheric electric field vectors attributable to these charges. **c** Ionospheric Hall (square) and Pedersen (cross) conductivity. **d** Ionospheric currents. **e** Up- (square) and downward (cross) field-aligned currents. **f** Equivalent currents on the ground; squares and crosses denote negative and positive Z components, respectively

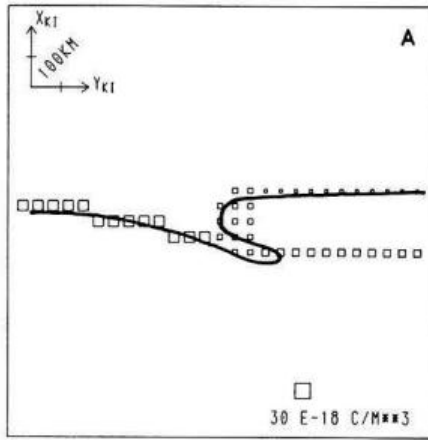
equivalent current is calculated using a Biot-Savart integration over the horizontal and field-aligned currents of all cells.

We initiate the modelling procedure by assuming a distribution of magnetic field-aligned columns of electrical charges above the ionospheric plane. The distribution of these column charges was to be simply related to the auroral form and consistent with the electric field pattern observed by STARE. Figures 5a and 6a show two different charge distributions that satisfy these criteria. In both cases negative charges are spread along the auroral form of the surge with an accumulation of column charges in the surge's head, this being necessary to create the eastward electric field component ahead of the surge. It was also found necessary to introduce a line of negative column charges along the eastward extension of the surge's hook in the southeast, in order to reduce the electric field magnitude east of the surge's head to sub-threshold values, as seen by STARE. The uncertainty of the electric field in this region gives rise to the two different models displayed in Figs. 5 and 6 (henceforth called models A and B). The two models differ with respect to the relative strength of the column charges north and south of the region of sub-threshold fields, east of the surge's head. Model A has, according to the luminosity distribution of the surge, the stronger column charges in the north

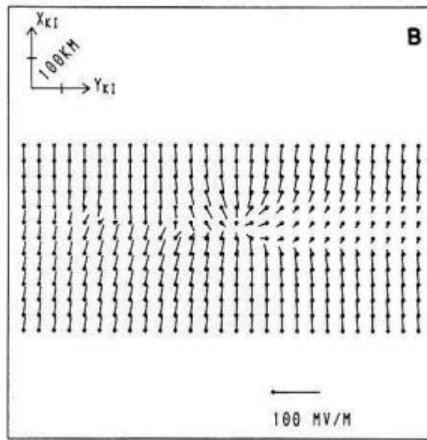
and consequently has a north-west directed electric field east of the surge of less than 15 mV/m in magnitude (see Fig. 5b). Model B has the stronger column charges along the southern border of that region, so that the southward electric field from the north can penetrate and gives rise to a sub-threshold, south-west directed electric field (see Fig. 6b). Thus both models give a westward electric field in the region east of the surge, as was to be expected, but differ with respect to the north-south component of the electric field in this region.

The variation of the ionospheric height-integrated conductivity was chosen such that the ionospheric current, following Ohm's law, together with the resultant field-aligned current distribution should reproduce the magnetic disturbances seen on the ground. Additional information is supplied from rocket measurements (Rème and Bosqued 1973; Meng et al. 1978), which have found a strong precipitation of energetic (>5 keV) electrons into the head and the region east of the surge. Restricting ourselves to a simple model, we therefore assumed homogeneously distributed height-integrated conductivities, except for the disturbed region of the surge's head and east of it. In order to find quantitative agreement between the modelled and the measured ground magnetic disturbances, we had to take a value of  $5.6 \Omega^{-1}$  for the un-

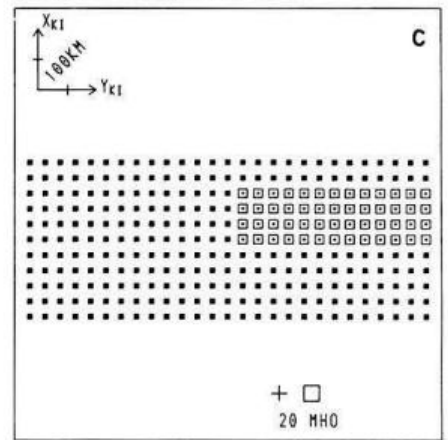
COLUMN CHARGES



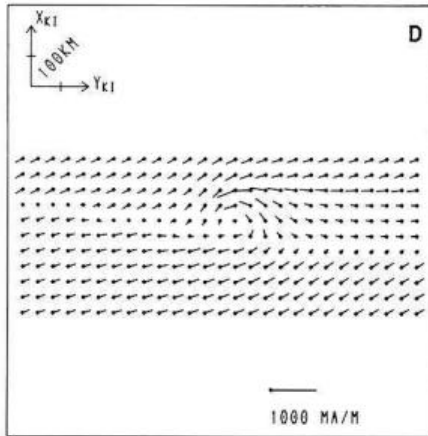
IONOSPHERIC ELECTRIC FIELD



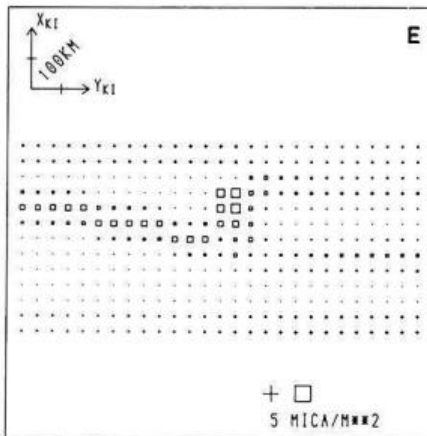
IONOSPHERIC CONDUCTIVITY



IONOSPHERIC CURRENTS



FIELD-ALIGN CURRENTS



EQ CURR GROUND

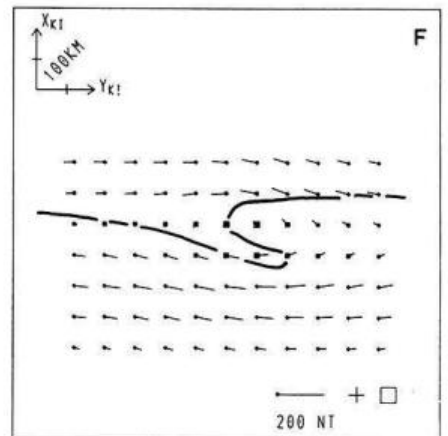


Fig. 6. Parameters of the model current system B and resultant equivalent current vectors on the ground; otherwise same as Fig. 5

disturbed height-integrated Hall conductivity and  $2.8 \Omega^{-1}$  for the Pedersen conductivity. Furthermore, we achieved consistency only if an enhanced Hall conductivity of  $11.2 \Omega^{-1}$  was assumed in the entire region of sub-threshold electric fields inside and east of the surge. For example, a Hall conductivity distribution that gradually decreases to the undisturbed conductivity from the surge's head towards east, does not reproduce the westward equivalent current flow measured behind the surge. The Pedersen conductivity in the disturbed region was set on the undisturbed value of  $2.8 \Omega^{-2}$ . As the model ground magnetic disturbances are insensitive to changes of the Pedersen conductivity in this region, this part of the model is somewhat uncertain within a factor of two. The variation of the conductivities used in the model calculation is shown in Figs. 5c and 6c. Basically, the assumed conductivity is in accord with measurements of electron density height-profiles by incoherent scatter radars. These show that in an undisturbed night time auroral ionosphere the height-integrated Hall conductivity varies from  $3-6 \Omega^{-1}$  and the ratio of  $\sum_H/\sum_P$  is about 2 (Banks and Doupnik 1975).

Figures 5d-f and 6d-f show the ionospheric height-integrated current resulting from Ohm's law, the field-aligned current density resulting from the divergence of the ionospheric current and the ground equivalent current calculated from the former by means of a Biot-Savart integration. Both models show eastward and westward current flow in the south and north, respectively, but the models have different currents in the region of enhanced con-

ductivity east of the surge. In model A, the eastward electrojet penetrates into this region and there are almost no field-aligned currents at the southern border of the region of enhanced conductivity. The electrical charges along the southern borderline, (see Fig. 5a) can, for this model, be consistently explained as polarisation charges which result when the north-eastward directed electrical current flow crosses the conductivity gradient. The resultant electric field difference on both sides of this borderline keeps the current flow divergence-free. If this model is correct, a net northward shift of the east-west current system should be observed after the passage of the surge. In model B, there is a westward current system behind the head of the surge, leading to an upward directed field-aligned current totalling  $4 \times 10^4$  A in the center of the surge. For the westward electrojet we find a total current of  $5.5 \times 10^4$  A, which is small compared with typical electrojet current strengths. Additionally, there are upward field-aligned currents along the northern and southern border of the region of enhanced conductivity, where we assumed negative electrical column charges. The second model clearly brings about an increase in the westward current flow after the passage of the surge.

A comparison of the model ground equivalent current systems with the measured equivalent currents in Fig. 4 shows clearly that model B is the more realistic one.

Model A does not reproduce the observed change from eastward to westward equivalent current flow, or the positive to negative  $A$  variation observed by a magnetometer station under-

neath the surge. Both of these features are observed in the equivalent current system of model B. The observed increase in the northward current flow east of the surge is also consistent with model B. In contrast, some details of the measured equivalent current system are not reproduced very well by model B. One feature is the very homogeneous eastward current south of the surge. We feel, that such details could be reproduced only if our assumed model were made more complex and that the necessary changes in the model would not bring about any basically new feature in the surge's current system.

## Discussion

In the preceding sections, we have presented data on the ionospheric electric field and ground equivalent current associated with a westward travelling surge. We have constructed a model for the three-dimensional current system, consistent with our data and previous measurements of the ionospheric electric field (Banks et al. 1973; Horwitz et al. 1978) as well as measurements of electron precipitation (Rème and Bosqued 1973; Meng et al. 1978) near a WTS.

This model (model B of the previous section, shown in Fig. 6) strongly supports the results of Rostoker and Hughes (1979), who identified the WTS with the intrusion of an upward field-aligned current, fed by the westward electrojet and the recent, more refined modelling of Tighe and Rostoker (in press 1981). As their models are based on ground magnetic observations alone, they propose ionospheric electric fields consistent with the current flow. This electric field is directed towards the south-east in a localised region inside and ahead of the WTS. Evidence for the existence of this field is obviously given by our measurements (see Fig. 4). East of the surge, Rostoker and Hughes (1979) assumed a south-west directed electric field, driving a westward current. The existence of this field can be verified only indirectly from our modelling and not directly by STARE, as the field was below the threshold of the STARE radar in this particular example. Incoherent scatter measurements (Banks et al. 1973; Horwitz et al. 1978) have shown that the electric field in this region has a westward component. In our case, a north-west directed electric field (as in model A of the previous section) has had to be discarded, as it does not lead to currents that reproduce our magnetic measurements, whereas a south-west directed electric field gives suitable agreement.

Another model for the surge's ionospheric current system has been proposed by Kisabeth and Rostoker (1973). They explained the ground magnetic variations observed during the passage of a surge as a step-like northward displacement of the westward electrojet. This displacement would be similar to the distortion undergone by a pre-existing auroral arc during the passage of the surge. They include no net field-aligned current in their model current system, and the westward electrojet flows further into the evening sector. Their model resembles somewhat our model A of the previous section with which our magnetic measurements are not in agreement.

An essential feature of the magnetic measurements in Kisabeth and Rostoker (1973) and Rostoker and Hughes (1979) is a positive  $D$  deflection under the head of the surge. The fact that we observe it only very weakly is no basic contradiction to Rostoker and Hughes' results. We could easily have produced a larger  $D$  deflection in our model, if we had extended the region of enhanced conductivity a little further to the west. In fact, Hughes and Rostoker (1979) assumed that a segment of the south-east directed electric field was located inside the head of the surge, whereas we measure it outside the region of auroral luminosity. The magni-

tude of the  $D$  deflection on the ground is therefore likely to depend critically on the correlation of the ionospheric electric field and the ionospheric conductivity near the head of the surge.

It may be quite interesting to relate the present results (model B of the previous section, shown in Fig. 6) to those reported by Baumjohann et al. (in press 1981) concerning a WTS in the process of being formed, i.e., local auroral breakups. These authors clearly showed that during the auroral breakup a strong southward directed polarisation field, caused by the high electrical conductivity associated with the active aurora, was superimposed on the quiet-time north-westward directed electric field, thus resulting in a total south-westward directed one in the breakup region. This is strikingly similar to what can be concluded from our observations and model calculations, i.e., during the passage of the WTS the previously northward directed electric field south of the auroral arc turned over to a south-westward direction, thus exhibiting the presence of a southward polarisation field in the higher conducting region. The polarisation charges at the boundaries of the higher conducting region (which are created by a northward Hall current driven by the westward electric field behind the surge's head) may be identified in Fig. 6a. Here, the negative charges at the northern boundary within the auroral structure are reduced (if compared to those ahead of the WTS) due to the presence of positive polarisation charges and negative polarisation charges can be seen at the southern boundary of the higher conducting region. Since in our case the conductivity enhancement and therefore the southward polarisation field is minor compared to that reported by Baumjohann et al. (1981), the westward Cowling current behind the surge is also comparatively weaker than the strong jetlike Cowling current observed by those authors.

*Acknowledgements.* We are greatly indebted to those past and present members of the magnetometer group at the University of Münster, who were involved in collecting the magnetic data. The magnetic observations were performed in cooperation with the Aarhus University, the Royal Institute of Technology at Stockholm, the Finnish Meteorological Institute at Helsinki, the University of Bergen, the Geophysical Observatory at Sodankylä, the Kiruna Geophysical Institute, the University of Oulu, and the University at Tromsø. We thank these institutions for their support. The STARE radars are operated in cooperation with ELAB and the Norwegian Technical University in Trondheim and the Finnish Meteorological Institute in Helsinki. We would like to thank T. Barilindhang and T. Rininen for their efforts in the everyday operation of the stations. Finally, we thank H. Maurer, T.U. Braunschweig, who supplied us with the magnetic data of the Braunschweig chain and R.J. Pellinen, FMI Helsinki, and H. Lauche, MPAE Lindau, who made the all-sky camera data available. The magnetometer array observations and the work of W. Baumjohann were supported financially by grants from the Deutsche Forschungsgemeinschaft. The work of R.A. Greenwald was supported in part by the Division of Atmospheric Sciences, National Science Foundation under grant ATM-8003300. We are grateful to G. Rostoker and another unknown referee for their instructive comments.

## References

- Akasofu, S.-I.: The development of the auroral substorm. *Planet. Space Sci.* **12**, 273–282, 1964
- Akasofu, S.-I., Meng, C.-I., Kimball, D.S.: Dynamics of the aurora – IV. Polar magnetic substorms and westward travelling surges. *J. Atmos. Terr. Phys.* **28**, 489–496, 1966
- Akasofu, S.-I., Eather, R.H., Bradbury, J.N.: The absence of the hydrogen emission ( $H\beta$ ) in the westward travelling surge. *Planet. Space Sci.* **17**, 1409–1412, 1969

- Banks, P.M., Doupnik, J.R.: A review of auroral zone electrodynamics deduced from incoherent scatter radar observations. *J. Atmos. Terr. Phys.* **37**, 951–972, 1975
- Banks, P.M., Doupnik, J.R., Akasofu, S.-I.: Electric field observations by incoherent scatter radar in the auroral zone. *J. Geophys. Res.* **78**, 6607–6622, 1973
- Baumjohann, W., Kamide, Y.: Joint two-dimensional observations of ground magnetic and ionospheric electric fields associated with auroral zone currents. 2. Three-dimensional current flow in the morning sector during substorm recovery. *J. Geomagn. Geoelectr.* **33**, in press 1981
- Baumjohann, W., Untiedt, J., Greenwald, R.A.: Joint two-dimensional observations of ground magnetic and ionospheric electric fields associated with auroral zone currents. 1. Three-dimensional current flows associated with a substorm-intensified eastward electrojet. *J. Geophys. Res.* **85**, 1963–1978, 1980
- Baumjohann, W., Pellinen, R.J., Opgenoorth, H.J., Nielsen, E.: Joint two-dimensional observations of ground magnetic and ionospheric electric fields associated with auroral zone currents. 4. Current systems associated with local auroral breakups. *Planet. Space Sci.* **29**, in press 1981
- Boyd, J.S., Belon, A.E., Romick, G.J.: Latitude and time variations in precipitated electron energy inferred from measurements of auroral height. *J. Geophys. Res.* **76**, 7694–7700, 1971
- Cahill, L.J. Jr., Greenwald, R.A., Nielsen, E.: Auroral radar and rocket double-probe observations of the electric field across the Harang-discontinuity. *Geophys. Res. Lett.* **5**, 687–690, 1978
- Ecklund, W.L., Balsley, B.B., Carter, D.A.: A preliminary comparison of F region plasma drifts and E region irregularity drifts in the auroral zone. *J. Geophys. Res.* **82**, 195–197, 1977
- Evans, D.S., Maynard, N.C., Trøim, J., Jacobsen, T., Egeland, A.: Auroral vector electric field and particle comparisons. 2. Electrodynamics of an arc. *J. Geophys. Res.* **82**, 2235–2249, 1977
- Farley, D.J.: A plasma instability resulting in field-aligned irregularities in the ionosphere. *J. Geophys. Res.* **68**, 6083–6097, 1963
- Greenwald, R.A., Weiss, W., Nielsen, E., Thomson, N.R.: STARE: a new radar auroral backscatter experiment in northern Scandinavia. *Radio Sci.* **13**, 1021–1039, 1978
- Gustafsson, G.: A revised corrected geomagnetic coordinate system. *Ark. Geofys.* **5**, 595–617, 1970
- Horwitz, J.L., Doupnik, J.R., Banks, P.M.: Chatanika radar observations of the latitudinal distributions of auroral zone electric fields, conductivities, and currents. *J. Geophys. Res.* **83**, 1463–1481, 1978
- Kamide, Y., Brekke, A.: Altitude of the eastward and westward auroral electrojets. *J. Geophys. Res.* **82**, 2851–2853, 1977
- Kisabeth, J.L., Rostoker, G.: Current flow in auroral loops and surges inferred from ground-based magnetic observations. *J. Geophys. Res.* **78**, 5573–5584, 1973
- Küppers, F., Untiedt, J., Baumjohann, W., Lange, K., Jones, A.G.: A two-dimensional magnetometer array for ground-based observations of auroral zone electric currents during the International Magnetospheric Study (IMS). *J. Geophys.* **46**, 429–450, 1979
- Maurer, H., Theile, B.: Parameters of the auroral electrojet from magnetic variations along a meridian. *J. Geophys.* **44**, 415–426, 1978
- Meng, C.-I., Snyder, A.L., Kroehl, H.W.: Observations of auroral westward travelling surges and electron precipitations. *J. Geophys. Res.* **83**, 575–585, 1978
- Rème, H., Bosqued, J.M.: Rocket observations of electron precipitation in a westward travelling surge. *J. Geophys. Res.* **78**, 5553–5558, 1973
- Rogister, A., D'Angelo, N.: Type II irregularities in the equatorial electrojet. *J. Geophys. Res.* **75**, 3879–3887, 1970
- Rostoker, G., Hughes, T.J.: A comprehensive model current system for high-latitude magnetic activity – II. The substorm component. *Geophys. J.R. Astron. Soc.* **58**, 571–581, 1979
- Tighe, W.G., Rostoker, G.: Characteristics of westward travelling surges during magnetospheric substorms. *J. Geophys.*, in press 1981

Received February 18, 1981; Revised Version March 20, 1981

Accepted March 23, 1981